

Transformation of the intensity profile for a step-index multimode fiber core

Shigeru Kobayashi^{1,2a)} and Okihito Sugihara²

¹ Tyco Electronics Japan G.K., Kawasaki 214–8533, Japan

² The Graduate School of Engineering, Utsunomiya University, 321–8585, Japan

a) skobayas@te.com

Abstract: The launch light conditions for the 200- μm core step-index multimode fiber have been defined by the International Electrotechnical Commission. However, we found conditions that give results outside the specified values, even when the launch lights are within the standardized encircled angular flux requirements. We report the transformation of the intensity profile for the fiber core showing non-uniform intensity distributions at practical link lengths. These distributions cause a gap compared to classical geometric models. We verified our proposed approach for a launch light study by using far- and near-field patterns of the fiber.

Keywords: EAF, encircled angular flux, launch light, step-index multimode fiber

Classification: Optical systems

References

- [1] M. Kagami, *et al.*: “Encircled angular flux representation of the modal power distribution and its behavior in a step index multimode fiber,” *J. Lightw. Technol.* **34** (2016) 943 (DOI: [10.1109/JLT.2016.2516644](https://doi.org/10.1109/JLT.2016.2516644)).
- [2] S. Kobayashi, *et al.*: “Launch light dependency of step-index multimode fiber connections analyzed by modal power distribution using encircled angular flux,” *Appl. Opt.* **56** (2017) 876 (DOI: [10.1364/AO.56.000876](https://doi.org/10.1364/AO.56.000876)).
- [3] Examinations and measurements — Encircled angular flux (EAF) measurement method based on two-dimensional far field data from step index multimode waveguide (including fibre), IEC 61300-3-53, Ed. 1.0 (2015).
- [4] R. Tao, *et al.*: “Equilibrium modal power distribution measurement of step-index hard plastic cladding and graded-index silica multimode fibers,” *Proc. SPIE* **9368** (2015) 93680N (DOI: [10.1117/12.2079355](https://doi.org/10.1117/12.2079355)).
- [5] K. Horiguchi, *et al.*: “Optical interface study of SI type PCS fiber for a gigabits network application,” *Proc. 64th Int. Wire Cable Symp. Conf.* (2015) 327.
- [6] S. Kobayashi and O. Sugihara: “Encircled angular flux: A new measurement metric for radiating modal power distributions from step-index multimode fibers,” *J. Lightw. Technol.* **34** (2016) 3803 (DOI: [10.1109/JLT.2016.2585577](https://doi.org/10.1109/JLT.2016.2585577)).
- [7] Fiber optic interconnecting devices and passive components — Basic test and measurement procedures, IEC 61300-1, Ed. 4.0 (2016).
- [8] M. Young: “Geometrical theory of multimode optical fiber-to-fiber connectors,” *Opt. Commun.* **7** (1973) 253 (DOI: [10.1016/0030-4018\(73\)90022-9](https://doi.org/10.1016/0030-4018(73)90022-9)).
- [9] W. van Etten, *et al.*: “Loss in multimode fiber connections with a gap,” *Appl. Opt.* **24** (1985) 970 (DOI: [10.1364/AO.24.000970](https://doi.org/10.1364/AO.24.000970)).

- [10] T. Iikubo, *et al.*: “Study on equilibrium mode distribution of HPCF,” IEICE Technical Report EMD 2013-2 (2013-05) (2013) 5.

1 Introduction

Step-index multimode fibers (SI-MMFs) are proven communication media for applications in harsh environments, such as factories and the automotive industry. There is a specific characteristic that must be considered when such fibers are used. Mode conversion of the propagating modal power distribution (MPD) easily occurs [1], and this phenomenon causes poor measurement reproducibility [2]. Although a sufficient margin of the link systems covers all variations, problems often occur with the components when their performances show variation in every measurement. Recently, the International Electrotechnical Commission (IEC) standardized the encircled angular flux (EAF) for defining the MPD in SI-MMFs [3]. Investigations on the behavior of the MPD in these fibers have progressed [2, 4, 5, 6]. We previously suggested the need for a launch light of component measurement for the 200- μm core step-index multimode fiber (i.e., A3e fiber of IEC 60793-2-30) to obtain better measurement reproducibility in [2].

In this paper, we report conditions that give results outside the specified values, even when the launch lights are within the standardized EAF requirements of the A3e fiber [7]. We present the transformation of the intensity profile for the fiber core as non-uniform distributions at fiber lengths of practical applications. We verified our approach for a launch light study by using the far-field pattern (FFP) and near-field pattern (NFP) of the fiber.

2 Experimental methods for launch light study

Fig. 1 shows the experimental setup for evaluating a single connection. We used a super-luminescent diode (SLD, Synos LSS002/850) with an 850 nm wavelength connected to the Gaussian beam-forming port of a launch beam-forming system (Synos M-Scope Type GR) that can seamlessly control the output Gaussian beam NA from 0.05 to 0.6 [2, 6]. The launch light from the launch beam-forming system was inserted into the input port of Fiber_A, which was replaced with several lengths of fiber from 1 m to 2000 m. As the device under test (DUT), the other side of Fiber_A and input port of Fiber_B (1 m length) were placed on each micropositioner, which could be aligned along the X- and Z-axes (i.e., lateral and axial directions). A3e fibers (OFS HCP-M0200T) with core and cladding diameters of 200 and

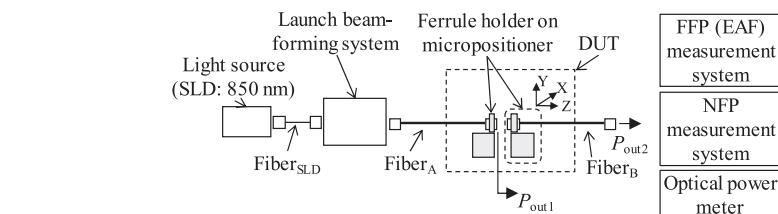


Fig. 1. Experimental setup for evaluating a connection.

230 μm , respectively, and a numerical aperture (NA) of 0.37 with a 500 μm coated diameter were used. All of the end-faces of these fibers were terminated with ferrules and polished to a flat and smooth finish [6]. Because we typically used this connection configuration with ferrules and a sleeve, the angular and lateral misalignments were limited [6]. The FFP and NFP of light radiated from the fibers were measured with the FFP and NFP measurement systems (Synos M-Scope Type F and Type I, respectively). EAF profiles were computed from the FFP data in the control computer [6]. In addition, we measured the output powers $P_{\text{out}1}$ (dBm) and $P_{\text{out}2}$ (dBm) from the fibers with a power meter. The insertion loss IL (dB) was calculated as $IL = P_{\text{out}1} - P_{\text{out}2}$.

3 Experimental and simulation results

3.1 Unexpected results

Fig. 2(a) shows the EAF requirements as the upper and lower bounds for the launch light of the A3e fiber [7] and the launch light EAF profiles at the point $P_{\text{out}1}$. The expected uncertainty was ± 0.2 dB, which is valid for attenuation values of ≤ 2.0 dB at a single connection when the measured EAF of the launch light is within the tolerance bounds [7]. These launch light profiles satisfied the EAF requirements located between the upper and lower bounds. LL is the light radiated from a 2000-m-long fiber, which was set as the equilibrium mode distribution (EMD) [6]. The beam NA of the Gaussian beam port was simply controlled with the launch beamforming system; A1, A2, and A3 refer to the upper, middle, and lower curves, respectively, of the light radiating from a 1-m-long fiber. Thus, we could generate launch lights that satisfied [7].

Fig. 2(b) plots the insertion loss dependency of the X- and Z-axis displacements of the DUT based on the launch light conditions in Fig. 2. The parameters x/a and z/a are the normalized displacements divided by the core radius $a = 100 \mu\text{m}$. A simulation was carried out by using the ray-tracing method (Zemax OpticStudio) with the fiber and connection parameters of the DUT and the FFP data of the light radiated from Fiber_A [2]. The experimental and simulation results for

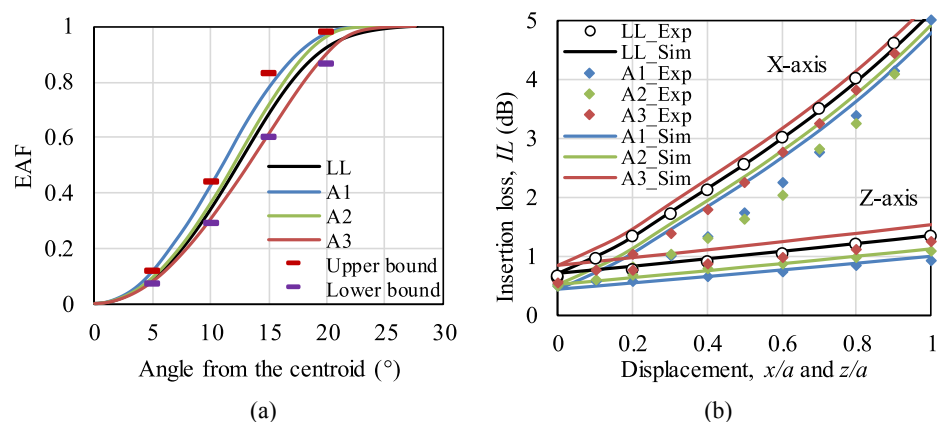


Fig. 2. (a) EAF profiles of the launch light with the input Gaussian beam NA of 0.5 at the point $P_{\text{out}1}$ and located within the upper and lower bounds of [7]. (b) Insertion loss results of the DUTs using the launch conditions of (a).

LL suggested that the simulation was appropriate because of their good agreement along both axes. However, A1 showed a 0.53 dB lower insertion loss in the experiment (1.31 dB) compared with the simulation result (1.84 dB) at $x/a = 0.4$, and A2 and A3 demonstrated the same tendency as A1. We found a condition outside the expected insertion loss and uncertainty results despite using a launch light that satisfied the EAF requirements of [7].

3.2 MPD transformation in NFP

The FFP data of LL and A1 were within the requirements for the launch light converted to the EAF profiles shown in Fig. 2(a). We measured the NFP profiles at the point P_{out1} using the fiber lengths of 2000 m (LL) and 1 m (A1) and show the two-dimensional (2-D) NFP images in Figs. 3(a) and (b), respectively, that were measured with an objective lens having an NA of 0.28. Fig. 3(a) shows a uniform intensity profile over the whole core area when light radiated from the 2000-m fiber, but Fig. 3(b) shows an intensity peak at the center of the core from the 1-m fiber using the input Gaussian beam NA of 0.5. Fig. 3(c) shows one-dimensional (1-D) NFP profiles outputted from fibers with different lengths of 1–2000 m and launched with a Gaussian beam NA of 0.5. The profiles became uniform as the fiber length increased. The unexpected result of a lower insertion loss may have been due to the non-uniform intensity distribution for the fiber core.

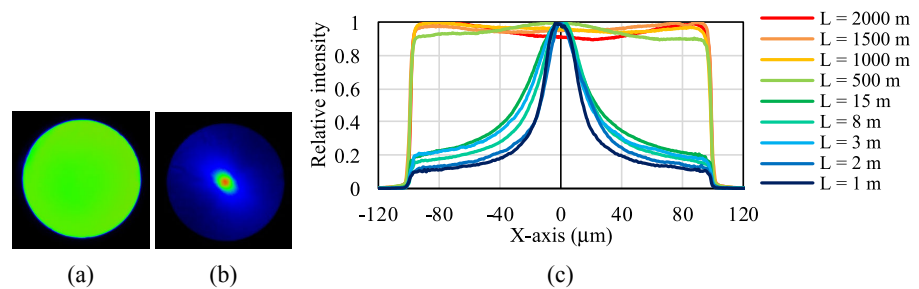


Fig. 3. 2-D NFP profiles of (a) $L = 2000$ m (EMD) and (b) $L = 1$ m, and (c) 1-D NFP profiles depending on the propagation length with the input Gaussian beam NA of 0.5.

3.3 Verification study of launch light

In order to clarify the relationship between NFP and FFP, the light outputted from a 3-m-long Fiber_A wrapped around a 10-mm-diameter rod ($\Phi 10$ mm) was investigated by using an input beam NA of 0.5. Figs. 4(a) and (b) show the 1-D NFP and 1-D FFP profiles, respectively, of the light at the point P_{out1} in Fig. 1. Fig. 4(a) shows that NFP reached an almost uniform distribution with three or more turns, although the profile of no turns showed an intensity peak at the center, like that in Fig. 3(b). Fig. 4(b) shows that the FFP profiles did not dramatically change under these wrapped conditions but became smoother as the number of turns increased.

Fig. 5(a) shows the launch light EAF profile outputted from the fiber wrapped five turns around the $\Phi 10$ -mm rod by using the input Gaussian beam NA of 0.5. This light satisfied the EAF requirements. Fig. 5(b) shows the measured insertion loss using the profile shown in Fig. 5(a) with variations in the NAs (0.05 and 0.6)

controlled with the launch beam-forming system in Fig. 1. Before this study, we confirmed that the Gaussian beam NAs of 0.55 and 0.6 also satisfied the EAF requirements. Their insertion losses were 1.55, 1.57, and 1.54 dB, respectively, at $x/a = 0.3$. These plots are overlapped each other in the range of the displacement, and these values are close to the value of 1.7 dB for LL and within the upper and lower simulation conditions of 1.89 and 1.45 dB at $x/a = 0.3$.

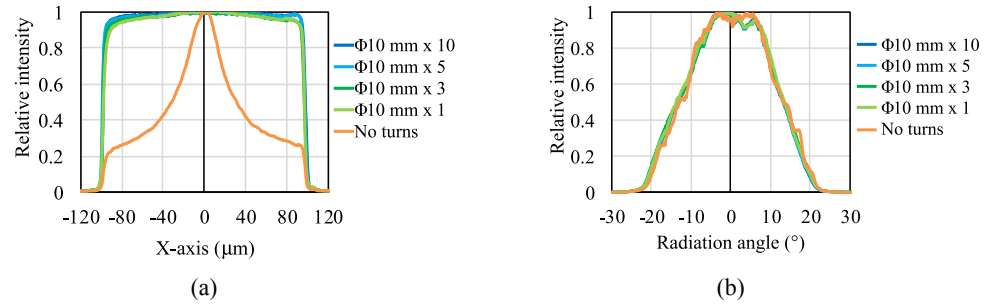


Fig. 4. Launch light outputted from a 3-m-long fiber using the input Gaussian beam NA of 0.5: (a) 1-D NFPs and (b) 1-D FFPs.

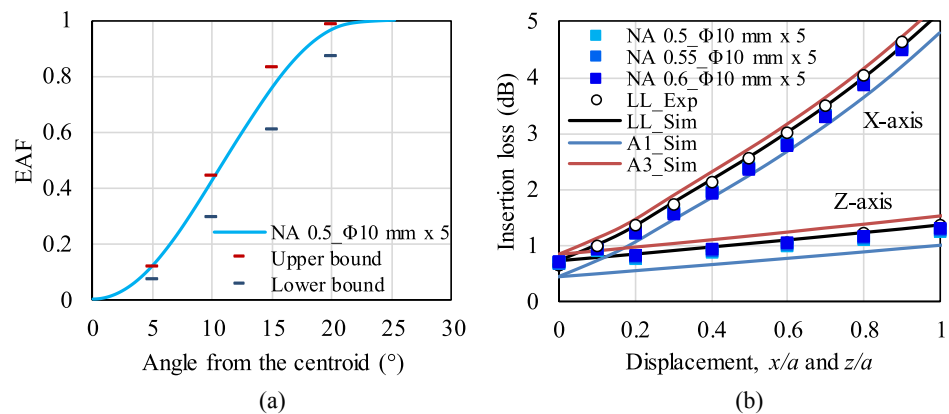


Fig. 5. (a) Launch light EAF profile with the input Gaussian beam NA of 0.5. (b) Insertion loss results using the launch light of (a) with variations of the NAs, 0.55 and 0.6. The reference insertion loss results were from using the EMD base launch light of LL and the upper and lower bounds of A1 and A3 from Fig. 2(b).

4 Discussion

We investigated the trend of NFP profiles for the SI-MMF reaching a uniform intensity profile distribution from the peak intensity profile at the center of the core as the fiber length increased. Because SI-MMFs have been typically discussed with FFP profiles, the ray-tracing simulation here also used only FFP data. However, these results are different from the experimental results and suggest the necessity of investigating NFPs in such a connection study. SI-MMFs have been used in short-reach data links using semiconductor light sources (e.g., NA of 0.2 for a vertical-cavity surface-emitting laser and NA of 0.4 or 0.5 for a light-emitting diode [6]) where the typical link length is several tens of meters or less. According to the

results of our study, those data link systems work with light propagation that has an intensity peak profile at the core center. The connection of SI-MMFs was the subject of a considerable number of studies until the 1980s. These studies typically used a geometric uniform distribution [8, 9] but did not consider the intensity peak at the center of the fiber core. Thus, here we revealed the cause of the gap in connection studies between the classical models and practical cases. Our future work will involve developing an analytical model from these results.

According to the launch light study, wrapping a fiber around a 10-mm-diameter rod effectively changed the axial intensity distribution of the output light, as shown by the NFP profiles in Fig. 4(a), but did not influence the angular distribution as given by the FFP profile in Fig. 4(b). Thus, the axial position of the optical path can be changed but not the reflective angle of the propagation light in the fiber. If we need to change the angular distribution of the propagation light, we may induce a large strain on the fiber to generate scattering [10].

We found conditions under which the insertion loss was not as expected, even though the use of the launch lights satisfied the standardized EAF requirements for an A3e fiber. Thus, there are two approaches for defining the launch light: adding NFP requirements in addition to the EAF requirements, or stating the method for generating the launch light, as we did in this study for example. In any case, further discussion is needed regarding the excessiveness of the EAF requirements because the light conditions of the EMD generated by a fiber that is 2000 m or longer are never used in practical cases [6].

5 Conclusion

We showed results outside the specified values, even when the launch lights were within the standardized EAF requirements of the 200- μm core step-index multimode fiber. We presented the transformation of the intensity profile for the fiber core, which reached a uniform intensity distribution as the fiber length increased. The results suggest that we typically use a non-uniform intensity distribution in practical cases. Thus, these results show that classical geometric models cannot be used in practical cases. We are working to establish an analytical model of the SI-MMF based on the results of the present study. We hope that our solutions contribute to industrial progress and ensuring the dissemination of technologies.

Acknowledgments

This work was supported in part by METI, Japan under the project “International standardization and dissemination project for high-speed communication network performance over large core multimode optical fiber—Technology integration for O-GEAR: Optical Gigabit Ethernet for Automotive aRchitecture”.